Development of a Micropatterned System to Study the Role of Protein Tethers in Lipid Membrane Organization

Samuel Lourenço Jacob
Centro de Química-Física Molecular & INESC-MN; Instituto Superior Técnico, Universidade de Lisboa, Lisbon, Portugal

ABSTRACT. The plasma membrane is a complex matrix of phospholipids and proteins that mediates important biological events. These events ultimately depend on the formation of lateral heterogeneities called membrane rafts. The plasma membrane interacts with the cytoskeleton, which is thought to help define and organize these rafts. Cytoskeleton adhesions to the membrane, such as those mediated by PIP_2, are thought to have a high impact on lipid distribution, especially if the membrane displays critical behavior. This work aimed to construct a model system that mimics cytoskeleton-PIP_2 tethers to the membrane. Making use of photolithography, we defined an avidin micropatterning on glass substrate; then, using supported lipid bilayers formed from liposomes containing biotinylated lipid, we attempted to study the effect of avidin-biotin binding in lipid phase separation and domain organization. Our optimization experiments showed that although formation of supported bilayers from small unilamellar vesicles onto the protein-coated surfaces did not occur, giant unilamellar vesicles (GUVs) adhered to an avidin surface and collapsed to form supported membranes as induced by osmotic shock. However, these giant liposomes were unable to adhere and form lipid bilayers onto an avidin micropatterned surface, possibly due to folding modifications occurring by organic solvent washing during microfabrication. Although the optimization of this model system is yet to be completed, the collapse of GUVs by osmotic shock on micropatterned protein surfaces is a promising tool to generate a model for the study of the interplay between membrane adhesions and lateral lipid domain formation.

Keywords: Membrane raft, phase separation, cytoskeleton, membrane adhesion, microfabrication, supported bilayers.

Introduction

The plasma membrane (PM) is present in all cells, not only delimiting the extracellular from the intercellular space and environment, but playing an important role in a variety of biological processes (1). Ever since the discovery of detergent-resistant membrane structures enriched in GPI-anchored proteins, cholesterol (Chol) and glycosphingolipids (2, 3), a number of studies have been performed confirming the existence of nanoscale lateral heterogeneities which were later called membrane rafts (4, 5) - these were associated with important biological events such as cell signaling, vesicular trafficking, exo and endocytosis and immunological synapses (3, 6, 7). At the 2006 Keystone Symposium, membrane rafts were defined: “Membrane rafts are small (10 - 200 nm), heterogeneous, highly dynamic, sterol- and sphingolipids-enriched domains that compartmentalize cellular processes. Small rafts can sometimes be stabilized to form larger platforms through protein-protein and protein-lipid interactions” (8). The existence of these heterogeneities in living cells has been associated with phase separation into liquid-ordered (L_o) and liquid-disordered (L_d) phases occurring in membrane model systems containing Chol and two types of lipid: one with a high and another with a low gel-fluid transition temperature (9, 10). The underlying physico-chemical principles that give rise to phase coexistence in artificial membranes have been thought to be the same as those that give rise to biological rafts (4, 11) and most studies have relied on these membranes containing mixtures of biologically relevant lipids. Temperature studies with giant plasma membrane vesicles (GPMVs) - cells separated from the influence of cytoskeleton and cell trafficking - highlighted that these membranes seemed to be made up of a single phase at high temperatures, but separated into two coexisting L_o- and L_d-like phases below a miscibility transition temperature (12). Further studies with GPMVs revealed that these undergo critical fluctuations near the miscibility transition temperature, suggesting that living cell membranes may have similar compositions, and thus be tuned to reside near miscibility critical points (13, 14). This conclusion lead many authors to speculate that lateral heterogeneities in the cell membrane (at physiological temperature) could correspond to critical fluctuations with dimensions below 50 nm (13).

On the other hand, cytoskeleton is currently considered an important component on membrane dynamics, and PM - cytoskeleton interactions have been associated with several biological processes in which membrane rafts also play a role (1, 15). In T cells, actin cytoskeleton was shown to be necessary in clustering raft components and forming the immunological synapse (7). Additionally, disparities in diffusion coefficients of lipids and transmembrane

proteins obtained in PM versus GPMVs and artificial membranes lead many authors to speculate that the cytoskeleton could be responsible for this behavior (16, 17). Kusumi et al. have proposed the fence-and-picket model to explain how the cytoskeleton organizes the cell membrane, suggesting that lipids and certain proteins are free to move within compartments of about 30 – 400 nm delimited by the actin cytoskeleton (18, 19).

One of the most important known PM – actin cytoskeleton interactions is through phosphatidylinositol 4,5-bisphosphate (PIP_2), which binds intermediate actin-binding proteins such as ezrin, radixin and moesin (ERM), thus providing an adhesion to the membrane (20, 21). Studies with this lipid have shown that it functions in membrane rafts mediating ABPs adhesions (22) and that it is necessary in T cell activation (23), although its influence on raft dynamics is still elusive.

Our current understanding of lateral heterogeneities in the plasma membrane embraces two main concepts: the concept of membrane rafts as near-critical composition fluctuations and the fence-and-picket model which provides a valuable framework to understand how the cytoskeleton organizes and distributes membrane heterogeneities. In the vicinity of a critical point, the presence of membrane adhesions, such as PIP_2-mediated cytoskeleton adhesions, is expected to dramatically influence phase separation (24) and this might be the physical basis behind the relevance of the cytoskeleton in several membrane raft-associated cellular functions. While most studies aiming to characterize the physical principles responsible for lateral heterogeneities in the plasma membrane have focused on spontaneous phase separation of biologically relevant lipid mixtures, few studies have attempted to characterize the direct effect of cytoskeleton adhesions in detail.

This project aimed to establish a new model system for the study of the impact of membrane adhesions on phase separation in artificial lipid membranes. This model was based on the tethering of supported lipid bilayers to an avidin-micropatterned glass surface through biotinylated lipid, thus mimicking, in a simple fashion, PIP_2-cytoskeleton tethers. Thereafter, using a novel approach, we pretended to conclude whether or not protein-membrane binding was sufficient to induce lipid domain formation and phase separation in biologically relevant membranes.

Materials and Methods

Materials and Reagents

Microscope glass coverslips with dimensions 24 mm x 50 mm and 0.17 mm thickness were obtained from Menzel-Gläser (Braunshweig, Germany). Hydrogen peroxide and sulfuric acid were obtained from Merck (Darmstadt, Germany). Avidin from egg white, albumin from bovine serum (BSA) and biotin-labeled albumin from bovine serum (BSA-biotin) were obtained from Sigma-Aldrich (St. Louis MO, USA). Avidin Alexa Fluor 488 conjugate (avidin-Alexa488) and avidin Alexa Fluor 350 conjugate (avidin-Alexa350) were purchased from Invitrogen (Breda, The Netherlands). PFR 7790G-27-cP positive photoresist and TMA238WA photoresist developer were obtained from JSR Micro (Leuven, Belgium). Hexamethyldisilazane (HDMS) was obtained from TCI America (Oregon, USA).

1-palmitoyl-2-oleoyl-*sn*-glycero-3-phosphocholine (POPC), 1,2-dioleoyl-*sn*-glycero-3-phosphoethanolamine-*N*-(cap biotinyl) (DOPE-cap-biotin) and lipid probes 1,2-dioleoyl-*sn*-glycero-3-phosphoethanolamine-*N*-(lissamine Rhodamine B sulfonyl) (Rhod-DOPE) and 1,2-dipalmitoyl-*sn*-glycero-3-phosphoethanolamine-*N*-(7-nitro-2-1,3-benzoxa-diazol-4-yl) (NBD-DPPE) were obtained from Avanti Polar Lipids (Alabaster, AL). All lipid solutions were kept in UVASOL grade chloroform, purchased from Merck (Darmstadt, Germany). All aqueous solutions in this project were prepared using MilliQ water.

Photolithography

All glass coverslips used were first rinsed in Piranha solution (H_2SO_4:H_2O_2, 3:1 v/v) during at least 2 hours, washed copiously with deionized water and dried under N_2 flux. These were submitted to a vapor priming process with HDMS during approximately 30 minutes, to promote subsequent photoresist adhesion. After this step, photoresist was spin-coated over the substrate at 2500 rpm and soft-baked at 85ºC to obtain a predicted thickness of ≈ 1.45 µm. Exposure of the regions to be later removed was done using direct write laser (DWL) lithography at 405 nm, performed by Lasarray 2.0 from Heidelberg Instruments (Heidelberg, Germany). Finally, the samples were baked at 110ºC, cooled and exposed to photoresist developer during 60 seconds, which removed previously light-exposed regions; the samples were finally washed with deionized water and dried. The treated glass coverslips were conserved at 4ºC before using, to minimize photoresist mask degradation (one week maximum).

Protein Immobilization and Micropatterning

Solutions of proteins (either avidin, BSA or BSA-biotin) to be immobilized in glass coverslips or glass bottom eight-well µ-Slides from Ibidi (Munich,

Germany), either avidin, BSA or BSA-biotin, were prepared at 0.1 or 1 mg/mL in pH 7.4 buffer containing 10 mM PBS, 1 M NaCl, 2.7 mM KCl and 50 µM NaN_3. Avidin-Alexa350 or avidin-Alexa488 were mixed with unlabeled avidin solution (1:12 or 1:25 mol:mol labeled to unlabeled protein ratio for either avidin-Alexa350 or avidin-Alexa488). 200 µL of the final protein solution was then added to the substrate and incubated for 1 hour; the substrate was washed in water and dried under N_2 flux.

To create the avidin micropatterning, coverslips containing photoresist were initially incubated with 200 µL BSA-biotin, washed abundantly with water, dried under N_2 flux and incubated with 200 µL avidin, followed by the same washing and drying step. The coverslips were rapidly washed with acetone to remove the photoresist and the overlying adsorbed protein, leaving only the BSA-biotin-avidin complex immobilized on the glass surface. The patterning was visualized by confocal or two-photon fluorescence microscopy.

Small Unilamellar Vesicles

Required volumes of lipid and fluorescent probe stock solutions were mixed in chloroform to the desired quantities. Simple POPC mixtures were prepared with either NBD-DPPE or Rhod-DOPE as membrane markers (at 1:200 and 1:500 mol:mol labeled to unlabeled lipid ratio, respectively). The lipid mixtures were then dried under N_2 flux, left in vacuum overnight and ressuspended in liposome hydration buffer (10 mM PBS, 150 mM NaCl, 3 mM KCl, pH 7.20). Sonication was performed on a Branson Sonifier 250 from Branson Ultrasonics (Danbury, USA) during 15 minutes to form small unilamellar vesicles (SUVs). After this step, the mixture was centrifuged using a Sigma 2K15 centrifuge from B. Braun (Melsungen, Germany) at 20000 g and 15ºC, during 30 minutes to remove particles from the sonifier microtip. The mixture was conserved at 4ºC until necessary. Before adding the SUVs to the glass coverslips, vesicles were diluted in liposome fusion buffer (10 mM HEPES, 150 mM NaCl, 3 mM NaN_3, 3 mM $CaCl_2$, pH 7.40) to 1 mM final lipid concentration. A 200 µL droplet was added to the substrate to form SLBs, and after one hour incubation, the samples were washed in liposome washing buffer (10 mM HEPES, 150 mM NaCl, 3 mM NaN_3, pH 7.40) to remove excess vesicles. An additional previously-treated glass coverslip was used to cover the substrate to prevent dehydration. The samples were visualized using confocal fluorescence microscopy.

Giant Unilamellar Vesicles

Giant unilamellar vesicles (GUVs) were obtained by electroformation using platinum wires as previously described (25). Required volumes of lipid and lipid fluorescent probe stock solutions were mixed in chloroform to the final concentration of 1 mM. Simple POPC mixtures included biotinylated lipid (DOPE-cap-biotin) at 1:1000 mol:mol labeled to unlabeled lipid ratio and either Rhod-DOPE or NBD-DPPE (1:500 or 1:200 mol:mol labeled to unlabeled lipid ratio) as a membrane marker. A total of 2 µL were spread over each electrode, which were subsequently emerged in 1 mL 200 mM sucrose solution pre-heated at 30ºC. Electroformation was performed at this temperature at 10 Hz frequency and 2 V amplitude during 75 minutes. The vesicles were then released into the solution by gently shaking the wires.

In order to increase the concentration of GUVs, a total of 4 or more electroformations were performed in the same conditions and GUV solutions were mixed together in a falcon tube to a total of 4 mL solution. An additional 4 mL of 200 mM glucose solution were added to the tube; the solution was incubated overnight in order to enrich vesicles in the bottom of the tube (as a result of the difference in density inside and outside the vesicles). Before using GUVs, a quantity and quality check was performed in uncoated eight-well µ-Slides from Ibidi (Munich, Germany) using confocal fluorescence microscopy. SLBs were formed by incubating 200 µL GUV solution plus 100 µL solution into either avidin-coated glass bottom eight-well µ-Slides from Ibidi (Munich, Germany) or avidin-coated glass coverslips during 1 hour, followed by removal of 200 µL solution and subsequent addition of the same volume of water to cause an osmotic shock and rupture of avidin-bound GUVs. The so formed SLBs were visualized by confocal fluorescence microscopy.

Confocal and Two-Photon Microscopy

All measurements were performed on a Leica TCS SP5 (Leica Microsystems CMS GmbH, Manheim, Germany) inverted confocal microscope (DMI6000). Excitation lines provided by an argon laser were focused into the sample by apochromatic immersion objectives, either 10x (0.4 numerical aperture) or 63x water objective (1.2 numerical aperture) from Zeiss (Jena, Germany); a pinhole of 1 airy unit (AU) was used to block out-of-focus signals. Two-photon excitation data were obtained using the same Leica TCS SP5 inverted microscope and objectives, but with a titanium-sapphire pulsed laser (Ti:Sa) as the excitation light source; in this case, since the two-photon focal volume is very small, pinhole diameter used was 600 µm to maximize emitted light collection.

In the first part of this work, to measure the quantity of avidin immobilized on glass, as well as to evaluate micropatterning, avidin-Alexa488 was excited by 488 nm argon laser line and fluorescence was collected between 500 - 650 nm. In the second and third part of this work, to measure the quantity of protein and quality of avidin micropatterning, avidin-Alexa350 was excited at 760 nm using Ti:Sa laser and fluorescence was collected between 400 - 460 nm. To study membrane organization and lipid distribution, NBD-DPPE and Rhod-DOPE were excited by a 488 nm and 514 nm argon laser lines, respectively. When used simultaneously, fluorescence from the NBD group was collected between 470 - 530 nm and fluorescence from the Rhod group was collected between 570 - 700 nm; when used separately, fluorescence from the NBD group was collected between 500 - 700 nm and fluorescence from the Rhod group was collected between 530 - 700 nm. To calculate intensity ratios between avidin-enriched regions and outside regions, background intensity was previously subtracted for each ROI defined. All analysis of imaging data was carried out using ImageJ software developed by Wayne Rasband (NIH, USA).

Fluorescence Recovery after Photobleaching

Fluorescence recovery after photobleaching (FRAP) measurements were performed on the same inverted confocal microscope based on FRAP image-based protocols (26). In all FRAP experiments, NBD-DPPE was excited at 488 nm and fluorescence was collected between 500 - 700 nm; Rhod-DOPE was excited at 514 nm and fluorescence was collected between 530 - 700 nm. Circular ROI for bleaching was defined with 2.5 µm radius in all experiments. The analysis of raw FRAP data was performed using FRAP Analyser software version 1.0.5 (http://actinsim.uni.lu/eng/). The intensity over time was first normalized, so that recovery curves become independent of initial values and fluorophore concentration (27, 28), using the double-normalization method represented in equation (1):

$$F_{norm}(t) = \left(\frac{F(t) - F_b(t)}{F_{prebleach}}\right)\left(\frac{F_{ref(prebleach)} - F_b(t)}{F_{ref}(t) - F_b(t)}\right) \quad (1)$$

Where $F(t)$, $F_{ref}(t)$, $F_b(t)$ are the average fluorescence intensity ($t < 0$) inside the bleached, referenced unbleached and background ROI, respectively. The "prebleach" subscript means the average fluorescence intensity before bleaching ($t \geq 0$) in the bleached or reference ROI. Using the normalized fluorescence, diffusion time was obtained by fitting a modified version of Soumpasis (29) to the experimental data:

$$F_{norm}(t) = a_0 + a_1 e^{-2\tau_D/t}\left[I_0\left(\frac{2\tau_D}{t}\right) + I_1\left(\frac{2\tau_D}{t}\right)\right] \quad (2)$$

Where $a_0 = F_{norm}(0)$ and $a_1 = F_{norm}(\infty) - F_{norm}(0)$; these terms are introduced to account for non-zero intensity at the bleach moment and incomplete recovery, respectively. τ_D is the characteristic diffusion time and I_0 and I_1 are Bessel functions. Finally, the lateral diffusion coefficient D can then be determined using equation (3):

$$D = \omega^2/4\tau_D \quad (3)$$

The mobile fraction, M_f, was then readily calculated using the equation (4):

$$M_f = \frac{F_{norm}(\infty) - F_{norm}(0)}{F_{norm_{(prebleach)}} - F_{norm}(0)} \quad (4)$$

In which $F_{norm_{(prebleach)}}$, $F_{norm}(0)$ and $F_{norm}(\infty)$ are the normalized fluorescence intensities before the bleach, immediately following the bleach ($t = 0$) and after full recovery ($t \to \infty$) (27).

RESULTS AND DISCUSSION

Formation of avidin micropatterning

We conceptualized a model to form discrete regions of avidin onto glass coverslips. These defined protein regions aimed to serve as adhesions to the membranes later formed onto glass, which would allow us to study the effect of these adhesions in phase separation and lipid distribution. The avidin micropatterning was created onto the glass substrate according to Materials and Methods. BSA-biotin and avidin were sequentially added to the previously formed photolithography mask. We observed that this step was efficient, since avidin-Alexa488 fluorescence was practically uniform everywhere, indicating that avidin immobilized both on photoresist and onto glass-exposed regions after binding BSA-biotin (Figure 1 - A). After washing with acetone, the photoresist was removed together with BSA-biotin and avidin adsorbed on it, forming a well defined pattern as it can be seen by the roman numeral and the 20 µm squares (Figure 1 - B). A small part of the pattern remained ill-defined, suggesting that BSA-biotin-bound avidin adsorbed onto the photoresist was not properly lifted-off during acetone washing step, resulting in either glass adsorption or binding to other complexes (avidin has 4 monomer subunits and BSA is conjugated with up to 16 biotin molecules, resulting in a high binding potential). Nevertheless, the definition of all three different squares sizes - 20, 10 and 5 µm – was successful, which was crucial to our work, since the accurate size of the tethers was an important feature to

define the model (Figure 1 - C, D, E). Perhaps one of the most important results was the high contrast observed between avidin-enriched regions and outside regions – it was essential that the outside of these regions contained little or no avidin, so as to minimize their impact on lipid organization. In fact, we compared Alexa488 emission spectrum outside and inside the avidin-enriched regions, concluding that no significant levels of avidin were present in the former, as opposed to the latter where the Alexa488 characteristic spectrum was detected (Figure 1 - F). Finally, we measured the absolute intensity of avidin-Alexa488 in several square regions, obtaining a ratio of intensities of approximately 98 between inside and outside regions, which was very satisfactory for the purpose of our work.

Due to the high intensity ratio obtained between avidin squares and outside regions, stability of the BSA-biotin and good pattern definition, the protocol here depicted was used in the subsequent studies of this work. The next experiment attempted to form these bilayers onto an avidin-micropatterned glass substrate.

Formation of supported lipid bilayers from POPC SUVs onto avidin micropatterned glass

The second part of the work aimed to elucidate whether a continuous SLB could be formed onto avidin micropatterned surface using a simple lipid mixture in the absence of liposome biotinylation. After the micropatterning was completed by standard procedure using BSA-biotin and avidin, we blocked one of the samples with BSA, while the other remained unblocked; in this way, BSA would be coating the glass regions outside the avidin-enriched regions and any effect observed inside these regions could be attributed to avidin and not to BSA. We used a mixture of POPC and NBD-DPPE as fluorescent probe.

In the sample without BSA blocking, results show

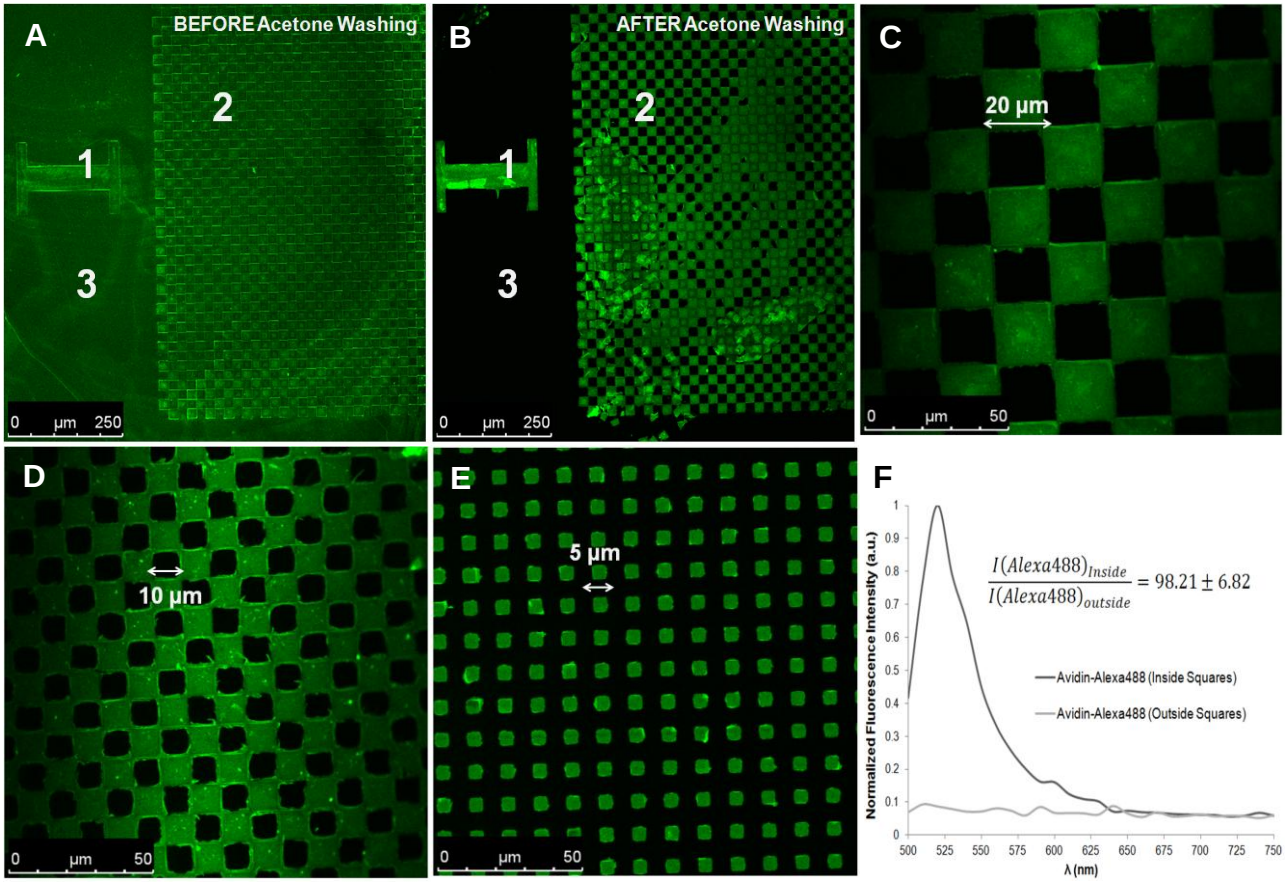

Figure 1 – Avidin micropatterning on glass coverslip. (A) Micropatterned surface after avidin addition and before acetone washing. Region 1 shows the numeral that identifies which pattern, out of nine possible patterns, was under observation. Region 2 shows the pattern, which is made of 20 µm squares; total protein-coated area is 50%. Region 3 represents the area outside the patterns, which was filled with photoresist and adsorbed BSA-biotin-bound avidin that would later be removed. Fluorescence can be seen everywhere, which indicates successful avidin immobilization on the surface. (B) Avidin micropatterning after acetone washing. Regions 1, 2 and 3 depicted are the same as in (A), except now BSA-biotin-bound avidin adsorbed onto photoresist got lifted-off; Alexa488 fluorescence revealed a well-defined avidin micropatterning. (C) Avidin micropatterning showing 20 µm squares (50% protein-coated area). (D) Avidin micropatterning showing 10 µm squares (50% protein-coated area). (E) Avidin micropatterning showing 5 µm squares (20% protein-coated area). Fluorescence is from avidin-Alexa488 (1:12 mol:mol labeled to unlabeled protein ratio). (F) Avidin-Alexa488 emission spectrum measured inside and outside avidin-enriched regions ($\lambda_{em\ peak} \approx 520$ nm); ratio of average fluorescence intensities inside and outside the same regions is also shown. BSA-biotin and avidin were added at 0.1 and 1 mg/mL concentration, respectively.

that the lipid was mainly present outside micropatterned regions, as indicated by ratio measurements (about 3 times more fluorescence intensity outside). This suggests that SUVs prefer the glass-exposed regions to the protein-coated areas (Figure 2 – A, B, C). Results for the sample where coverslip exposed areas were blocked with an additional 0.1 mg/mL BSA show, on the other hand, that NBD-DPPE co-localized with avidin-enriched regions, as indicated by imaging and intensity ratios (about 13 times more intense inside avidin regions) (Figure 2 - D, E, F). Since we used a POPC mixture, which had no potential to phase separate, NBD-DPPE enrichment in these regions was surely not related to lipid mixture and phase separation; additionally, biotinylated lipid is absent from the experiment and no membrane component was expected to have affinity towards these regions. These results seem to suggest that the inclusion of avidin in the surface strongly promotes the adsorption of SUVs to the protein surface when compared to BSA, likely as a result of the different electrostatic properties of avidin and BSA. FRAP experiments were then performed both in the control and in BSA-coated micropatterned surfaces to verify if a continuous SLB was present or absent in the sample.

FRAP results for the control sample (without BSA blocking) show that a continuous supported lipid membrane existed, in some regions, outside the avidin regions (Figure 2 – G), indicating that this surface does not prevent formation of SLBs from SUVs even after micropatterning procedure. All lipid was mobile with diffusion coefficient of 0.84 ± 0.08 $\mu m^2/s$, which is slightly lower than the previously obtained in non-micropatterned glass (1.30 ± 0.22 $\mu m^2/s$, results not shown) and lower than literature (1.80 ± 0.20 $\mu m^2/s$ obtained for Rhod-DOPE on a glass-supported POPC membrane (30)). This difference in diffusion might have to do with (i) the substrate, which in this case is modified during the micropatterning procedure, rendering the surface more hydrophobic and affecting lipid mobility when compared with clean glass; (ii) an incomplete membrane, which lead to an underestimation of the diffusion coefficient.

On the other hand, results for the BSA-blocked surface show the presence of both a mobile (17% of total lipid) and an immobile (83%) fraction of labeled lipid on the SLB within avidin-coated regions (Figure 2

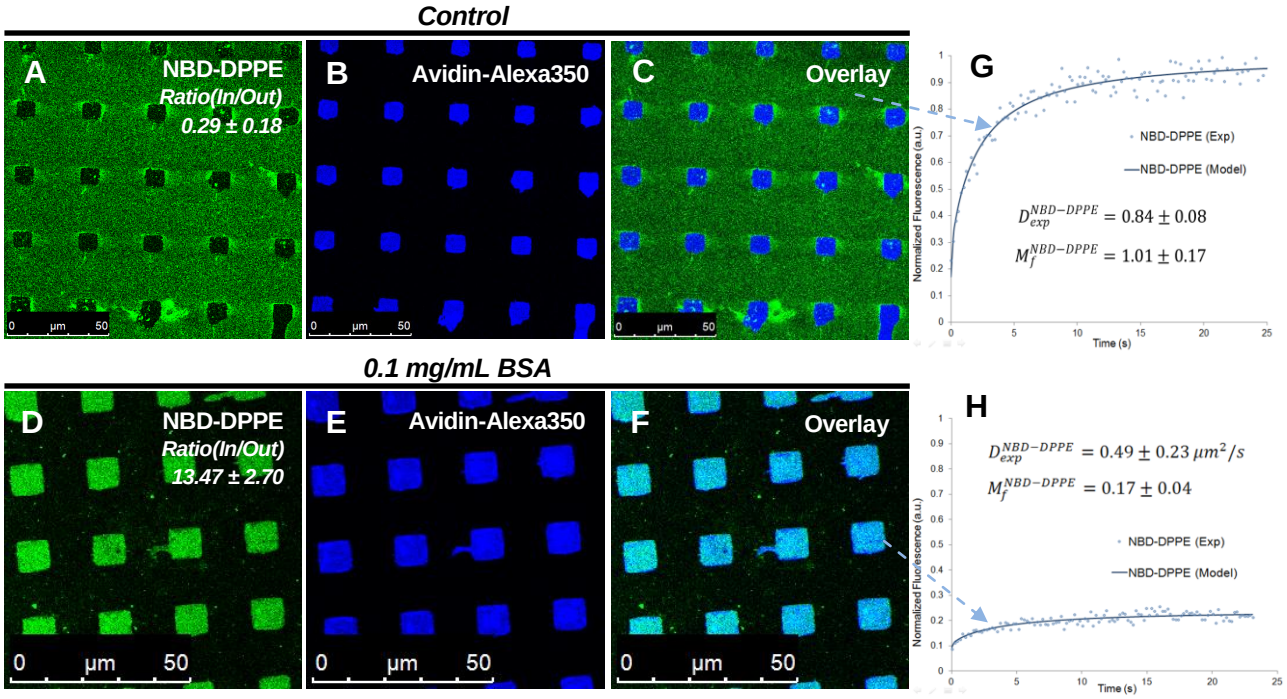

Figure 2 – Effect of avidin micropatterning on the formation of supported lipid bilayers from POPC SUVs. (A), (B), (C) Avidin micropatterning showing NBD-DPPE fluorescent signal, avidin-Alexa350 fluorescent signal and overlay between the two for the sample not blocked with BSA; exclusion of NBD-DPPE from avidin-enriched regions was observed. (D), (E), (F) Avidin micropatterning showing NBD-DPPE fluorescent signal, avidin-Alexa350 fluorescent signal and overlay between the two for the sample blocked with additional 0.1 mg/mL BSA; NBD-DPPE signal is enriched in avidin-enriched regions. (G), (H) FRAP curve (normalized fluorescence over time) for NBD-DPPE outside the avidin-enriched regions (in glass) for the sample not blocked with BSA and inside avidin-enriched regions in BSA-blocked sample, respectively. Diffusion coefficient *D* and mobile fraction M_f are also shown. NBD-DPPE and avidin-Alexa350 were used at 1:200 and 1:12 labeled to unlabeled lipid and protein ratio, respectively. Avidin pattern was fabricated on glass coverslips according to Materials and Methods. BSA-biotin and avidin were added at 1 mg/mL concentration and BSA was added at 0.1 mg/mL concentration.

– H). The mobile lipid population diffused with a diffusion coefficient of D = 0.49 ± 0.23 μm^2/s. The low diffusion coefficient obtained could be explained by defective membranes which impaired normal lateral lipid diffusion. Identical results for the mobile fraction were obtained for these regions in samples not blocked with BSA (not shown), suggesting that SLBs cannot properly form onto avidin-enriched regions.

We performed several tests attempting to force SLB formation onto protein-coated surfaces, including the use of high temperature and PEG, which proved unsuccessful (results not shown). Thus, it was confirmed that with the standard methods it was not possible to form SLBs in a protein-coated surface. The next studies aimed to optimize a different method of forming SLBs that did not rely on SUVs, but rather made use of giant unilamellar vesicles (GUVs).

Formation of supported lipid bilayers from POPC GUVs onto avidin-coated and micropatterned glass substrate

The diameter of giant unilamellar vesicles typically exceeds several micrometers (31), making them less stable than SUVs vesicles when tethered to a surface. We pretended to make use of GUVs, which would adhere to the avidin-coated surface and eventually collapse, forming SLBs. We performed four electroformations of GUVs containing POPC and biotinylated lipid (DOPE-cap-biotin), two of them with Rhod-DOPE and the other two with NBD-DPPE as a membrane fluorescent label. The GUV solution was added to an Ibidi glass bottom slides previously coated with BSA-biotin and avidin.

Imaging results under the confocal microscope showed GUVs independently labeled with Rhod-DOPE or NBD-DPPE immobilized on the surface (Figure 3 – A). After 1 hour rest, we tried to induce an osmotic shock onto these vesicles. We carefully removed 200 μL of solution from the chamber, added the same amount of glucose/sucrose free water and immediately observed the results under the microscope, observing that most of the GUVs had collapsed, forming SLBs (Figure 3 - B); osmotic shock proved to be an effective strategy to collapse to form SLBs from GUVs. In fact, we observed the existence of supported bilayers containing both NBD-DPPE and Rhod-DOPE signals (Figure 3 - B); since GUVs were formed with either fluorescent label separately, this could be attributed to membrane fusion from GUVs labeled with Rhod-DOPE and NBD-DPPE after rupture. This is important, since it means that larger membranes can be formed by fusion of two or more smaller membranes. To verify lipid probe mobility in the SLBs, we chose a membrane labeled with only NBD-DPPE or Rhod-DOPE and performed FRAP studies. We obtained a diffusion coefficient of 1.50 ± 0.24 μm^2/s for NBD-DPPE and 2.10 ± 0.22 μm^2/s for Rhod-DOPE, both in agreement with literature (30). For both probes, we obtained a mobile fraction of 100%, showing a properly-formed membrane onto avidin-coated glass surface (Figure 3 – C, D).

The next studies focused on forming SLBs from GUVs on avidin micropatterning by the same methodology used in Ibidi glass bottom slides. When the mixture was added to an avidin micropatterned glass coverslip, GUVs were observable even before osmotic shock (results not shown); however, after inducing the osmotic shock, no SLBs were apparently detected and GUV size seemed to decrease (Figure 3 - E; the red spots that can be seen on the surface belong to the lower part of the vesicles close to the surface; the plane of the GUVs is above the micropatterning and is not shown). Additionally, most of the GUVs were not immobilized, contrarily to what happened in normal avidin-coated surfaces, where they were readily immobilized. Thus, the behavior of GUVs onto the avidin micropatterning, when comparing with a non-micropatterned surface, seems to suggest that these vesicles are not binding surface avidin after micropatterning fabrication. The decreasing size of non-immobilized GUVs after osmotic shock could be explained by minimization of osmotic stress by fission.

The last studies tried to elucidate why GUVs were unable adhere to avidin micropatterned surfaces by evaluating the direct effect of acetone on GUV immobilization in a BSA-biotin and avidin non-micropatterned surface. For this, we performed four electroformations of GUVs containing POPC and DOPE-cap-biotin with Rhod-DOPE as membrane label; we did not use the GUV concentration procedure described in Materials and Methods, since we did not require high quantities of vesicles for the purpose of this experiment. Ibidi glass bottom slides coated with BSA-biotin and avidin were either briefly washed with acetone and water or only with water. We added the GUV solution to the Ibidi glass bottom slides and waited one hour to let the vesicles deposit in the bottom of the surface. The results show that, as expected, GUVs immobilized and collapsed to form SLBs in the control sample even before osmotic shock (Figure 3 – F). On the contrary, the sample washed with acetone after protein incubation was not able to immobilize and form SLBs; the red spots that can be seen on the surface belong to the lower part of the vesicles close to the surface (Figure 3 – G).

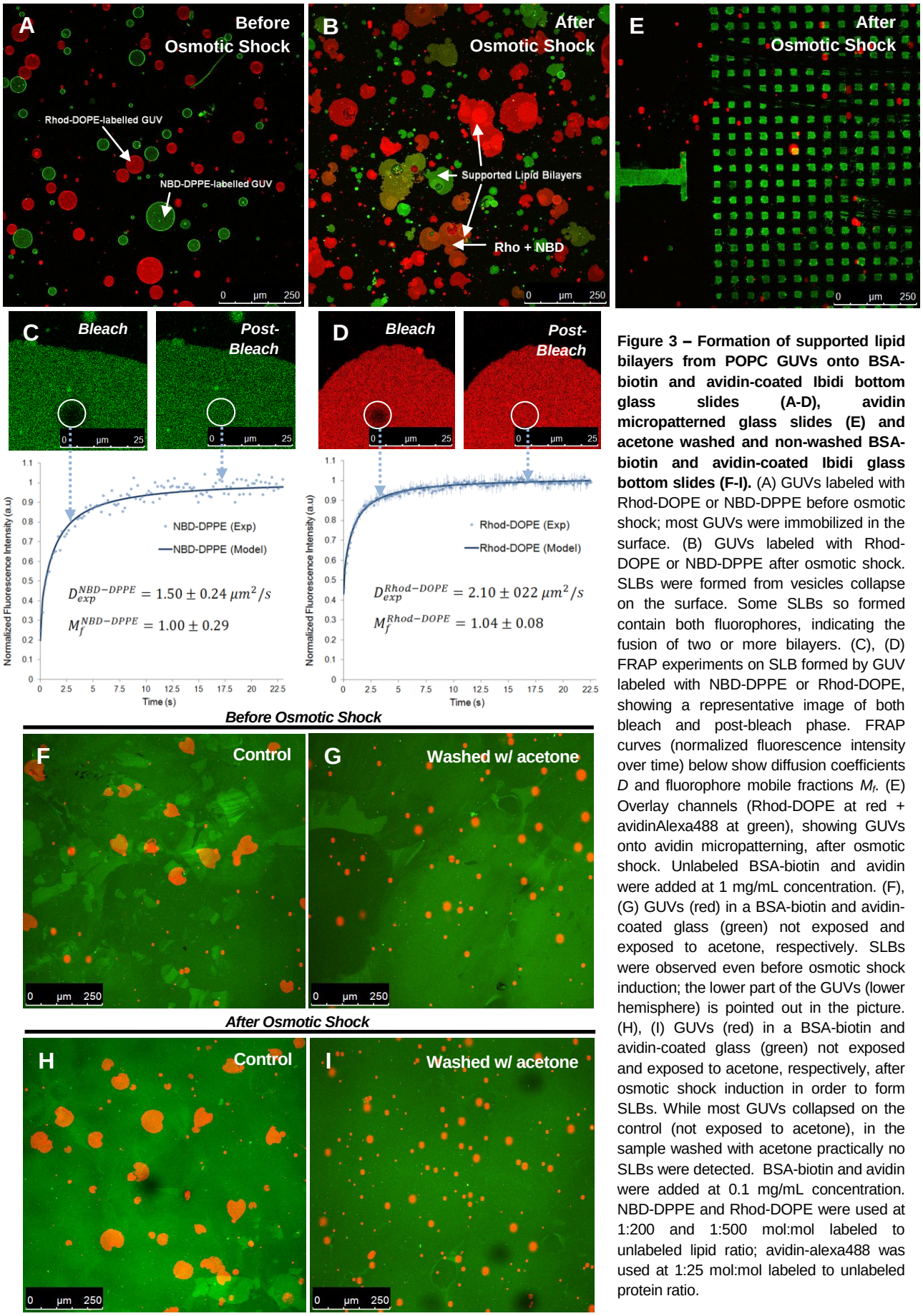

Figure 3 – Formation of supported lipid bilayers from POPC GUVs onto BSA-biotin and avidin-coated Ibidi bottom glass slides (A-D), avidin micropatterned glass slides (E) and acetone washed and non-washed BSA-biotin and avidin-coated Ibidi glass bottom slides (F-I). (A) GUVs labeled with Rhod-DOPE or NBD-DPPE before osmotic shock; most GUVs were immobilized in the surface. (B) GUVs labeled with Rhod-DOPE or NBD-DPPE after osmotic shock. SLBs were formed from vesicles collapse on the surface. Some SLBs so formed contain both fluorophores, indicating the fusion of two or more bilayers. (C), (D) FRAP experiments on SLB formed by GUV labeled with NBD-DPPE or Rhod-DOPE, showing a representative image of both bleach and post-bleach phase. FRAP curves (normalized fluorescence intensity over time) below show diffusion coefficients *D* and fluorophore mobile fractions M_f. (E) Overlay channels (Rhod-DOPE at red + avidinAlexa488 at green), showing GUVs onto avidin micropatterning, after osmotic shock. Unlabeled BSA-biotin and avidin were added at 1 mg/mL concentration. (F), (G) GUVs (red) in a BSA-biotin and avidin-coated glass (green) not exposed and exposed to acetone, respectively. SLBs were observed even before osmotic shock induction; the lower part of the GUVs (lower hemisphere) is pointed out in the picture. (H), (I) GUVs (red) in a BSA-biotin and avidin-coated glass (green) not exposed and exposed to acetone, respectively, after osmotic shock induction in order to form SLBs. While most GUVs collapsed on the control (not exposed to acetone), in the sample washed with acetone practically no SLBs were detected. BSA-biotin and avidin were added at 0.1 mg/mL concentration. NBD-DPPE and Rhod-DOPE were used at 1:200 and 1:500 mol:mol labeled to unlabeled lipid ratio; avidin-alexa488 was used at 1:25 mol:mol labeled to unlabeled protein ratio.

After osmotic shock induction, practically all the vesicles had burst to form SLBs on the surface of the control, while none had done this on the sample washed with acetone (Figure 3 – H, I).

The results suggest that acetone is responsible for the inability of avidin to bind biotinylated lipids on GUVs, shedding light on why these vesicles were unable to bind to the avidin micropatterned surface; partial denaturation of avidin during the acetone washing step is a strong possibility. However, these results do not explain why previous experiments with biotin-fluorescein conjugate showed that this molecule was able to efficiently bind the micropatterned surface and retain this ability even after acetone washing (results not shown). One could try to explain these results suggesting that biotin-fluorescein can bind surface avidin much easier than biotin when inserted in a GUV – the former is a small molecule that can easily diffuse through aqueous solution, while the latter is inserted in a large membrane, having a much lower diffusion rate and more difficult access for binding.

Final Remarks

The formation of SLBs onto a protein micropatterned surface fabricated by standard photolithography is a challenging task.

On one hand, SUVs are the most appropriate systems for studies attempting to form SLBs on clean glass, but fail to form defective-free and homogeneous bilayers onto protein-coated surfaces. In fact SUVs are shown here to be highly stable when immobilized in a BSA-biotin/avidin coated surface. It is possible that this property is useful for applications demanding presentation of liposomes in surfaces.

On the other hand, GUVs are far more unstable when immobilized than SUVs, even in protein-coated surfaces. We then employed GUVs as tools for the generation of SLBs. The attempt to form supported bilayers from GUVs onto BSA-biotin and avidin coated surfaces was successful, since after osmotic shock induction practically all immobilized GUVs were able to form homogeneous membranes, and even fuse with each other to create larger membranes; in principle, the size of membranes so created would be enough for us to study the effect of avidin adhesions on membranes with a composition that enabled phase coexistence to occur. However, GUVs proved unable to adhere to the avidin micropatterned surface, an effect that we ultimately attributed to the acetone washing step. This effect was not expected for two main reasons: first, biotin fluorescein experiments showed that acetone washing had no effect on the ability of avidin to bind biotin in solution; second, we observed that SUVs containing biotinylated lipid still bound micropatterned avidin, suggesting that this protein was not affected after acetone washing (results not shown). After acetone washing, proteins in the surface might be modified such that only small molecules such as biotin, or small vesicles, are able to efficiently bind avidin, while bigger-sized vesicles, such as GUVs, are incapable of doing so. In this way, it is clear that, in order to achieve SLB formation with GUVs on micropatterned surfaces, avidin must not be exposed to this type of treatment.

A possible alternative is to perform incubation of BSA-biotin-patterned surfaces with avidin only after acetone treatment, making sure that non-specific adsorption of avidin to the exposed coverslip surface is kept at a minimum.

Alternative methods that rely on photomasks include the use of photosensitizes that graft desired proteins on PEG surfaces or the use of deep-UV that selectively destroys binding molecules through oxidation (32, 33). However, most lithographic procedures still have the problem of low biocompatibility. One of the most widely used techniques for biological applications that require protein micropatterning is soft lithography, namely microcontact printing using a PDMS stamp, which is a potential future strategy to create the avidin micropatterning due to its high biocompatibility (32, 34).

Altogether, it is evident that merging a delicate field of study such as biophysics with microtechnologies proves challenging, since these fields were born from radically different backgrounds and are, in the broadest, concerned with different goals. Additionally, the plasma membrane of living cells is so complex that it is almost imperative to study its principles and dynamics at a more simple level. The cytoskeleton, as already stated, is likely to be an extremely important component in mediating the formation of plasma membrane heterogeneites (such as membrane rafts), and there is a great need to include adhesions to the lipid membrane *in vitro* and observe what the effects are in relevant lipid mixtures able to display phase coexistence. The completion of the work is a worthy and important goal to pursue, and it is the source of much motivation for future studies.

References

1. Head, B.P., H.H. Patel, and P. a Insel. 2014. Interaction of membrane/lipid rafts with the cytoskeleton: impact on signaling and function: membrane/lipid rafts, mediators of cytoskeletal arrangement and cell signaling. Biochim. Biophys. Acta. 1838: 532–45.

2. Schroeder, R., E. London, and D. Brown. 1994. Interactions between saturated acyl chains confer detergent resistance on lipids and glycosylphosphatidylinositol (GPI)-anchored proteins: GPI-anchored proteins in liposomes and cells show

similar behavior. Proc. Natl. Acad. Sci. U. S. A. 91: 12130–4.

3. Brown, D.A. 2006. Lipid rafts, detergent-resistant membranes, and raft targeting signals. Physiology. 21: 430–9.

4. Lingwood, D., and K. Simons. 2010. Lipid rafts as a membrane-organizing principle. Science. 327: 46–50.

5. Simons, K., and J.L. Sampaio. 2011. Membrane organization and lipid rafts. Cold Spring Harb. Perspect. Biol. 3.

6. Simons, K., and E. Ikonen. 1997. Functional rafts in cell membranes. Nature. 387: 569–72.

7. Meiri, K.F. 2005. Lipid rafts and regulation of the cytoskeleton during T cell activation. Philos. Trans. R. Soc. B. 360: 1663–72.

8. Pike, L.J. 2006. Rafts defined: a report on the Keystone symposium on lipid rafts and cell function. J. Lipid Res. 47: 1597–8.

9. Feigenson, G.W. 2007. Phase boundaries and biological membranes. Annu. Rev. Biophys. Biomol. Struct. 36: 63–77.

10. Heberle, F.A., and G.W. Feigenson. 2011. Phase separation in lipid membranes. Cold Spring Harb. Perspect. Biol. 3.

11. García-Sáez, A.J., and P. Schwille. 2010. Stability of lipid domains. FEBS Lett. 584: 1653–8.

12. Baumgart, T., A.T. Hammond, P. Sengupta, S.T. Hess, D. a Holowka, et al. 2007. Large-scale fluid/fluid phase separation of proteins and lipids in giant plasma membrane vesicles. Proc. Natl. Acad. Sci. U. S. A. 104: 3165–70.

13. Veatch, S.L., O. Soubias, S.L. Keller, and K. Gawrisch. 2007. Critical fluctuations in domain-forming lipid mixtures. Proc. Natl. Acad. Sci. U. S. A. 104: 17650–5.

14. Veatch, S.L., P. Cicuta, P. Sengupta, A. Honerkamp-Smith, D. Holowka, et al. 2008. Critical fluctuations in plasma membrane vesicles. ACS Chem. Biol. 3: 287–93.

15. Doherty, G.J., and H.T. McMahon. 2008. Mediation, modulation, and consequences of membrane-cytoskeleton interactions. Annu. Rev. Biophys. 37: 65–95.

16. Fujiwara, T., K. Ritchie, H. Murakoshi, K. Jacobson, and A. Kusumi. 2002. Phospholipids undergo hop diffusion in compartmentalized cell membrane. J. Cell Biol. 157: 1071–81.

17. Sako, Y., A. Nagafuchi, S. Tsukita, M. Takeichi, and A. Kusumi. 1998. Cytoplasmic regulation of the movement of E-cadherin on the free cell surface as studied by optical tweezers and single particle tracking: corralling and tethering by the membrane skeleton. J. Cell Biol. 140: 1227–40.

18. Ritchie, K., R. Iino, T. Fujiwara, K. Murase, and A. Kusumi. 2003. The fence and picket structure of the plasma membrane of live cells as revealed by single molecule techniques (Review). Mol. Membr. Biol. 20: 13–18.

19. Kusumi, A., T.K. Fujiwara, R. Chadda, M. Xie, T.A. Tsunoyama, et al. 2012. Dynamic organizing principles of the plasma membrane that regulate signal transduction: commemorating the fortieth anniversary of Singer and Nicolson's fluid-mosaic model. Annu. Rev. Cell Dev. Biol. 28: 215–50.

20. Saarikangas, J., H. Zhao, and P. Lappalainen. 2010. Regulation of the actin cytoskeleton-plasma membrane interplay by phosphoinositides. Physiol. Rev. 90: 259–89.

21. Zhang, L., Y.S. Mao, P.A. Janmey, and H.L. Yin. 2012. Phosphatidylinositol 4, 5 bisphosphate and the actin cytoskeleton. Subcell. Biochem. 59: 177–215.

22. Rozelle, A.L., L.M. Machesky, M. Yamamoto, M.H. Driessens, R.H. Insall, et al. 2000. Phosphatidylinositol 4,5-bisphosphate induces actin-based movement of raft-enriched vesicles through WASP-Arp2/3. Curr. Biol. 10: 311–20.

23. Johnson, C.M., G.R. Chichili, and W. Rodgers. 2008. Compartmentalization of phosphatidylinositol 4,5-bisphosphate signaling evidenced using targeted phosphatases. J. Biol. Chem. 283: 29920–8.

24. Bagatolli, L.A., J.H. Ipsen, A.C. Simonsen, and O.G. Mouritsen. 2010. An outlook on organization of lipids in membranes: searching for a realistic connection with the organization of biological membranes. Prog. Lipid Res. 49: 378–89.

25. De Almeida, R.F.M., J. Borst, A. Fedorov, M. Prieto, and A.J.W.G. Visser. 2007. Complexity of lipid domains and rafts in giant unilamellar vesicles revealed by combining imaging and microscopic and macroscopic time-resolved fluorescence. Biophys. J. 93: 539–53.

26. Waharte, F., K. Steenkeste, R. Briandet, and M.-P. Fontaine-Aupart. 2010. Diffusion measurements inside biofilms by image-based fluorescence recovery after photobleaching (FRAP) analysis with a commercial confocal laser scanning microscope. Appl. Environ. Microbiol. 76: 5860–9.

27. Ishikawa-Ankerhold, H.C., R. Ankerhold, and G.P.C. Drummen. 2012. Advanced fluorescence microscopy techniques--FRAP, FLIP, FLAP, FRET and FLIM. Molecules. 17: 4047–132.

28. Phair, R.D., S.A. Gorski, and T. Misteli. 2004. Measurement of dynamic protein binding to chromatin in vivo, using photobleaching microscopy. Methods Enzymol. 375: 393–414.

29. Soumpasis, D.M. 1983. Theoretical analysis of fluorescence photobleaching recovery experiments. Biophys. J. 41: 95–7.

30. Guo, L., J.Y. Har, J. Sankaran, Y. Hong, B. Kannan, et al. 2008. Molecular diffusion measurement in lipid bilayers over wide concentration ranges: a comparative study. Chemphyschem. 9: 721–8.

31. Sezgin, E., and P. Schwille. 2012. Model membrane platforms to study protein-membrane interactions. Mol. Membr. Biol. 29: 144–54.

32. Théry, M. 2010. Micropatterning as a tool to decipher cell morphogenesis and functions. J. Cell Sci. 123: 4201–13.

33. Azioune, A., N. Carpi, Q. Tseng, M. Théry, and M. Piel. 2010. Protein micropatterns: A direct printing protocol using deep UVs. Methods Cell Biol. 97: 133–46.

34. Whitesides, G.M., E. Ostuni, S. Takayama, X. Jiang, and D.E. Ingber. 2001. Soft lithography in biology and biochemistry. Annu. Rev. Biomed. Eng. 3: 335–73.